RSC Advances

ROYAL SOCIETY OF CHEMISTRY

www.rsc.org/advances

Journal Name

RSCPublishing

ARTICLE

Xylene sensor based on α-MoO_3 nanobelts with fast response and low operating temperature

Cite this: DOI: 10.1039/x0xx00000x

Dingsheng Jiang[a], Ying Wang[a], Wei Wei[b], Feng Li[a], Yujia Li[b], Linghui Zhu[a], Caihui Feng[b], Caixia Liu[b,*], Shengping Ruan[a,*]

Received 00th January 2012,
Accepted 00th January 2012

DOI: 10.1039/x0xx00000x

www.rsc.org/

Hydrothermal treatment strategy was used to synthesize α-MoO_3 nanobelts. X-ray diffraction (XRD), scanning electron microscopy (SEM) was used to characterize the phase and the morphology of the samples. The result shows the length and the width of α-MoO_3 nanobelts is about 6μm and 200 nm, respectively. The sensing properties towards various kinds of gases were tested and the heater-type sensors coated with α-MoO_3 nanobelts showed excellent performance towards xylene. The sensors achieved a response of 3 to 100 ppm xylene at an operating temperature of 206 °C. The response and recovery time is 7 s and 87 s respectively.

Introduction

Xylene mainly comes from chemical engineering materials such as painting and adhesive in the indoor environment, even microscale of xylene has tremendous damage to human being. And careless oral of xylene can cause acute pneumonia and cancer. So it is significant to detect and measure the existence and content of xylene. Hitherto, various effective methods, such as solid-state chemical technology[1], micro fabricated preconcentrator[2] technology, double-layered metal-oxide thin film technology[3] have been used to detect xylene. However, these methods have disadvantages of slow response speed, bulky machine and danger to body, etc. Metal oxide semiconductor demonstrates the advantages of low cost, facile method, easy fabrication, fast response and recovery time.

Various materials such as $Co_3O_4$and $In_{2-x}Ni_xO_3$were used to detect xylene and exhibited excellent preferment[1, 3-5]. However, they are not satisfactory in response time towards xylene. Thus the improvement in response is urgently needed to detect xylene.

α-MoO_3 has been investigated and applied in solar cell[6-9], catalyst[10-13], capacitors[14-16], light-emitting diodes[17, 18], gas sensors and optical detectors. In recent years,α-MoO_3has been one of the most newly-developing n-type metal oxide semiconductors which can detect toxic gas. α-MoO_3 is an n-type semiconductor with a wide band gap of 3.2 eV and has been investigated for NO_2[19], ethanol[20], TMA[21], H_2S[22],H_2[23], and C_2H_5OH[24] detection. However, there is no report for xylene detection using α-MoO_3nano structure until now.

One dimensional (1D) nanostructure oxide semiconductors such as nanotubes, nanowires, nanofibers and nanobelts have received much attention due to the high ratio of surface to volume. Plenty of methods such as electrospinning, vapor-solid and hydrothermal synthesis were used to prepare 1D nanostructure materials during the past decades. One-dimension nano-products play an important role in gas sensing owing to the advantages of high surface. High ratio of surface to volume can achieve higher response comparing with that of low ratio.

In this study, optimum experiment condition of synthesizing α-MoO_3 nanobelts was researched via a facile hydrothermal method at a low temperature of 180 °C. The gas sensing properties based on α-MoO_3 nanobelts materials were investigated for detecting xylene. Heater-type sensors based on α-MoO_3 nanobelts performed excellent response as well as fast response time to xylene at a low operating temperature of 206 °C which is lower than that of most other sensors[1, 5, 23, 25].

Experimental

Synthesis of α-MoO_3 nanobelts

All of the chemical reagents are analytical grade and without any further purification. In a typical experimental procedure0.618g of ammo-nium heptamolybdate tetrahydrate ($(NH_4)_6Mo_7O_{24}\cdot 4H_2O$) was dissolved into 25 ml of deionized water with continuous stirring to achieve aqueous solution(0.02 M). Then 2.5 ml of nitric acid (HNO_3) was slowly dropwise-added into the aqueous solution. After stirring, the solution was transferred into a Teflon-lined stainless steel autoclave of 50 ml capacity with hydrothermal treatment for 12/24/36/48 hat 120 °C and 12/24/36/48 h at 180 °C to explore the optimum condition of the reaction, respectively. After the autoclaves were cooled down to room temperature, white precipitation was separated by centrifugation with deionized water and ethanol for 5 times. Then the precipitation was dried at 60 °C for 12 h. Finally the products were annealed at 300 °C for 2 h at the speed of 1°C/min to obtain the light yellow α-MoO_3 nanobelts.

Characterization

X-ray diffraction patterns were achieved to measure the phase identification and the crystal sizes (Rigaku TTRIII X-ray diffractometer with Cu Kα 1 radiation (λ=1.5406 Å) in the range of 20-80°). The morphologies of the samples were achieved by scanning electron microscopy (JEOL JSM-7500F microscope operating at 15 kV).

Fabrication and measurement of gas sensors

Sensor devices were fabricated by the similar method in our previous work[4, 26].The prepared products were mixed with deionized water at a weight ratio of 1:4 and grinded for a while. Then the specimens were coated on the surface of the ceramic tube which was attached with a pair of parallel golden electrodes using a small brush. The Ni-Cr alloy heating coil was inserted through the ceramic tube. The structure of sensors is showed in fig.1.

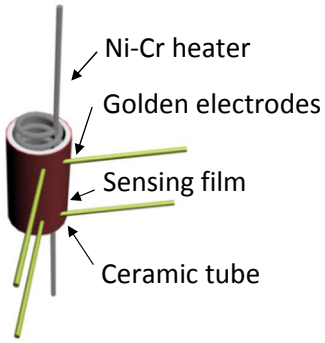

Fig. 1 structure of heater-type gas sensor after coating sensing film

The working temperature was measured by electric current which were produced by CGS-8 Intelligent Gas Sensing Analysis System(Beijing Elite Tech Co., Ltd., China). The test gases were injected by micro injections from air bags. The response of the gas sensors was expressed and measured as R_a (the resistance of the sensors in the air) /R_g (the resistance of the sensor in test gas). The response time is defined as the period in which the resistance of sensors reach from 10 % to 90 % of the steady value when exposed to test gases, while the recovery time is defined as the period in which the resistance of sensors reach from 90 % to 10 % of the steady value after exposed to oxygen.[27]

Result and discussion

Materials characterizations

Fig.2(A-H) shows the morphologies of the samples which were calcined at 300 °C for 2hafterhydrothermal treatment for 12/24/36/48 h at 180 °C and 12/24/36/48hat 120 °C, respectively. As shown in Fig.2(E,F,G,H), the morphologies of the samples were needle like with hydrothermal treatment for12/24/36/48 h at 120°C. The morphologies in Fig.2(A,B,C,D) show that nanobelts were achieved in hydrothermal treatment for 12/24/36/48 h at 180 °C. Fig. 2(D) shows that the nanobelts formed the phenomenon of agglomeration and the uniformity of the Fig.2(C) are better than Fig. 2(A, B), so the following discussions are reference to hydrothermal treatment for 36 h at 180 °C. The width of the α-MoO_3 nanobelt was about 200 nm, and the length was about 6μm.

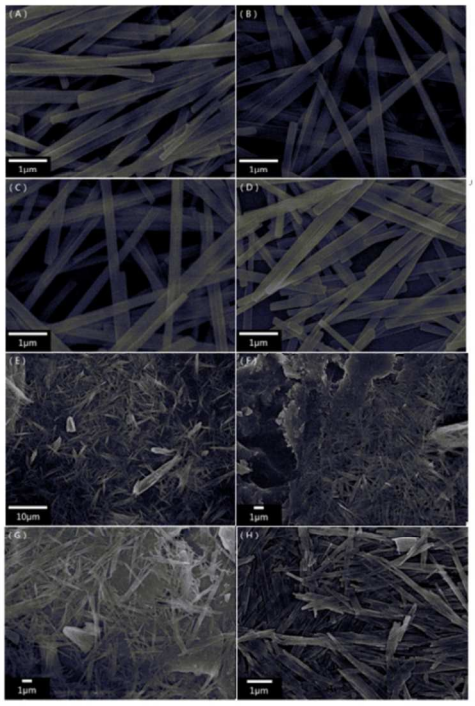

Fig. 2 (A-H) SEM images of pure α-MoO_3 nanostructure for 12/24/36/48 h at 180 °C and for 12/24/36/48 h at 120°C, respectively

The phase identification and the crystal sizes of the prepared materials were investigated by X-Ray Diffraction. Fig.3 shows the XRD patterns of the specimens which were calcined at 300 °C. The sample was assigned to pure α-MoO_3 (JCPDS 05-0508) by verifying the patterns of the sample.

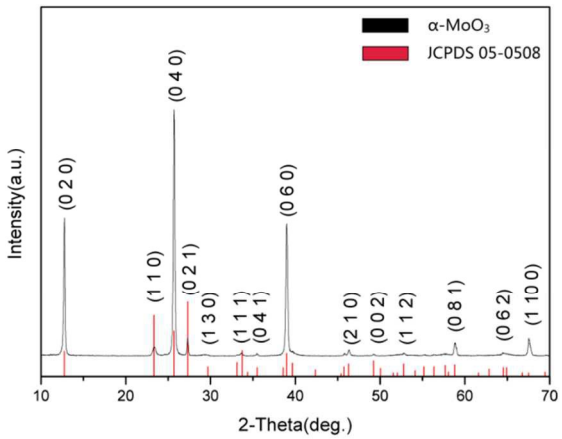

Fig. 3 XRD patterns of pureα-MoO_3 nanostructure after calcination for 2 h at 300°C

Gas sensing properties

The sensors which were coated with α-MoO_3 nanobelts had a good performance on xylene. In order to find the optimum

temperature of the sensors, the responses of the sensors to 100 ppm xylene at different temperatures were collected. As showed in Fig.4, the response increased along with the working temperature from 136 °C to 206 °C. It was obvious that the temperature improved the chemical reaction between sensors and test gas because it increased the speed of molecule vibration. However, further increase in temperature resulted in the response of the sensors decreasing. The reason illustrated in Fig.5 shows that chemical reaction between xylene and α-MoO_3 nanobelts was so fast that the penetration was less relative to the whole sensing film. Thus, the response of the sensor decreased along with temperature. Therefore, the response reached maximum value of 3 when temperature was 206 °C.

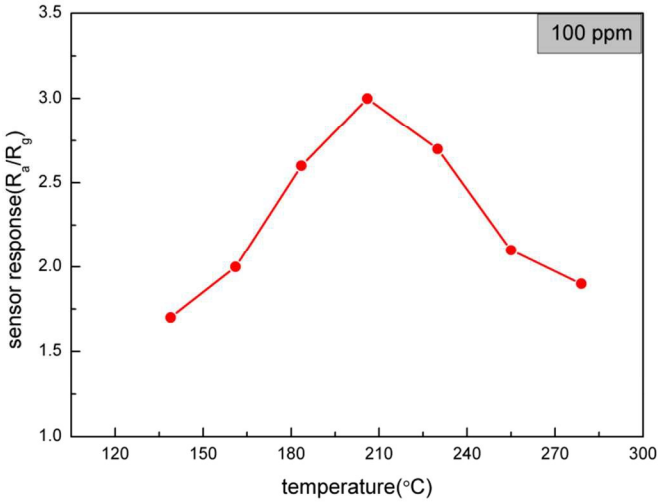

Fig. 4 response of sensors based onα-MoO_3nanobelts to 100 ppm xylene at different temperature

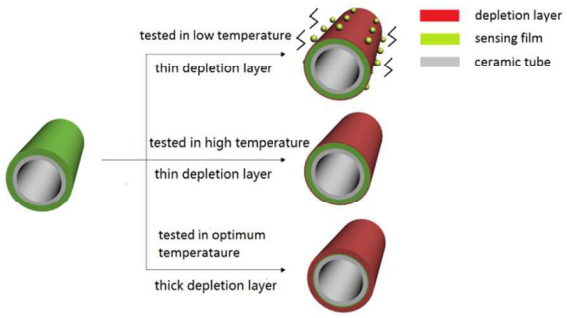

Fig. 5 illustration of optimum temperature of sensors based on α-MoO_3 nanobelts

Fig.6 shows the response of the sensors towards different concentrations of the test gas (xylene) at 206 °C. The response increased nearly linearly with the concentration of xylene at the range of 5 to 100 ppm and came to saturation when the concentration is over 1000 ppm. Significantly, the response of the sensor could reach 1.89 towards xylene at 5 ppm.

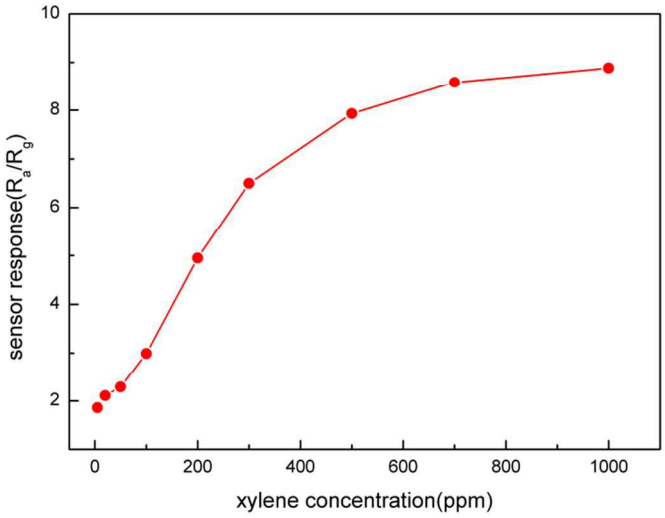

Fig. 6 response of sensors based on α-MoO_3 nanobelts at 206 °C versus concentration of xylene

Selectivity is an important property of gas sensors in the practical application. The responses of the sensors towards different test gases such as methylbenzene, formaldehyde and carbon monoxide were showed in Fig.7. The gases were tested at 206 °C with a concentration of 100 ppm similarly. The result shows that the response of the sensors based on α-MoO_3 nanobelts to 100 ppm of xylene could reach 3 and to other test gases were less than 1.6. The sensors also showed a low response towards other tested gases at different temperature including toluene. Therefore, α-MoO_3 has a good selectivity to xylene. However, it is still difficult for us to distinguish the three forms of xylene(o,m,p) at present because of their similar chemical properties.

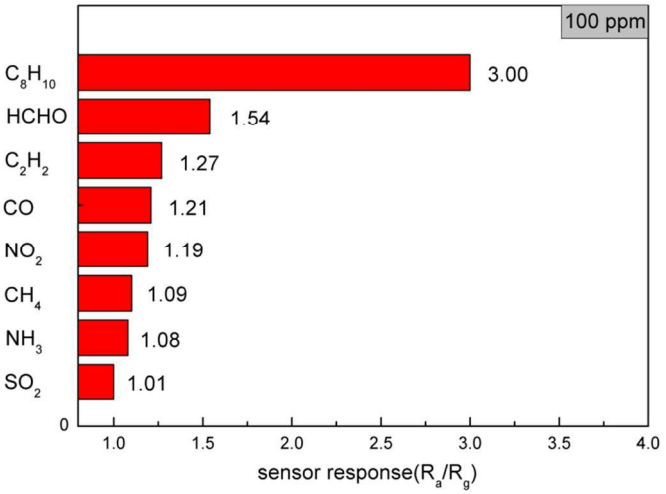

Fig. 7 response of sensors based on α-MoO_3 nanobelts at 206 °C towards various test gases

Rapid response and recovery time are significant parameters in designing oxide semiconductor gas sensors. Fig.8 shows the response and recovery characters of the sensors towards xylene from 20 ppm to 100 ppm at 206 °C. The figure indicated that

the resistance of the sensors decreased rapidly at first and then changed slowly due to the reaction slowed down gradually when the sensors were transferred from air to xylene. The resistance of the sensors resumed slowly when sensors were exposed to the air. The time of response and recovery were 7 s and 87 s, respectively. The fast response may be due to high ratio of surface to volume of 1D nanostructure.

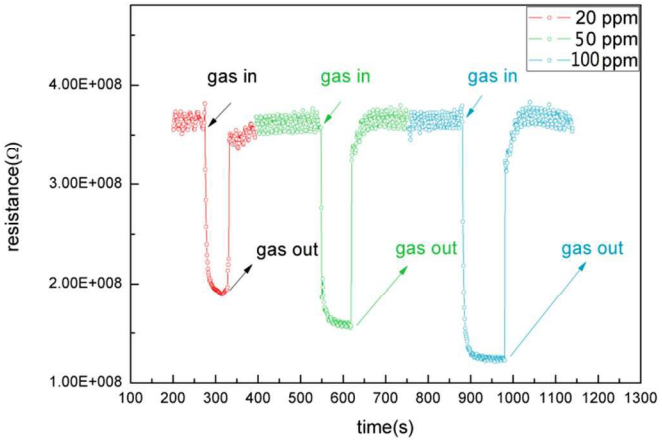

Fig. 8 response to different concentration of xylene for α-MoO_3 nanobelts at 206 °C

Sensing mechanism ofα-MoO_3nanobelts to xylene

As a n-type semiconductor, the sensing performance of α-MoO_3 nanobelts maybe related to the mechanism of adsorption and desorption process of gas molecules on the surface of the oxide because of crystal structure[28]. As shown in Fig. 9, the formation of defects in α-MoO_3 nanobelts is as following: The oxygen is attached on the α-MoO_3 nanobelts when the sensor is exposed in air. The oxygen captures electrons from α-MoO_3 nanobelts and transforms into O^-(420K-670K), O^{2-}(above 670K), and O_2^- (below 420K) on the surface of sensing layer which would lead the holes spread all over the surface of α-MoO_3 nanobelts and the resistance increasing[28]. When the α-MoO_3 nanobelts are transformed to the test gas (xylene), the interaction between xylene and the adsorbed oxygen ions can be explained as following:

$C_8H_{10} + 21O^- \rightarrow 8CO_2 + 5H_2O + 21e^-$ (420 K-670 K) (1)

$C_8H_{10} + 21\ O^{2-} \rightarrow 8CO_2 + 5H_2O + 42\ e^-$(above 670 K) (2)

$2C_8H_{10} + 21\ O_2^- \rightarrow 16CO_2 + 10H_2O + 21e^-$(below 420 K) (3)

$e^- + h^\circ \rightarrow$ Null (4)

Because the optimum temperature of the sensors based on α-MoO_3 nanobelts is 206°C(479 K), the reaction including O^-as shown in equation (1) was the dominative form in the process. Oxygen ion would release CO_2 and electrons when the reaction processing. These electrons neutralize the holes in the α-MoO_3 nanobelts and cause the decreasing of the resistance of the sensors. The excellent sensing performance makes α-MoO_3 nanobelts a newly potential candidate for the detection of xylene.

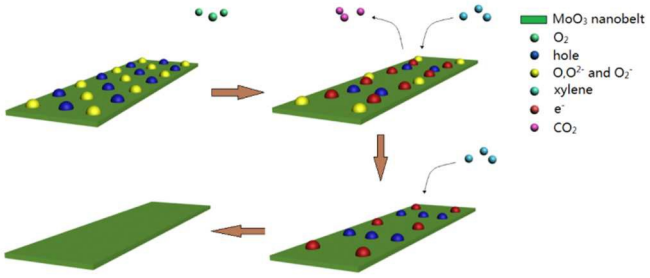

Fig. 9 illustration of sensors based on α-MoO_3 nanobelts sensing performance for xylene

The fast response of the sensors based on α-MoO_3 nanobelts materials could be attributed to the 1D nanostructure. The ratio of length and width of α-MoO_3 nanobelts could reach as high as 30/1 and the nanobelts were pretty thin, which leads the adsorption and desorption of O_2 and xylene faster at the surface of the sensing layer. Consequently, reaction occurred at sensing surface will be greatly accelerated, which results in faster response of the sensors based on α-MoO_3 nanobelts.

Conclusions

In conclusion, the optimum condition of synthesizing α-MoO_3 nanobelts was explored successfully by hydro-thermal method. The α-MoO_3 nanobelts were homogeneous and thin with width of 200 nm and length of 6 μm. Sensors based on α-MoO_3 nanobelts exhibited a fast response of 7 s and recovery time of 87 s. The sensors showed a high response for xylene at a low operating temperature of 206 °C. The result shows that α-MoO_3 nanostructure is a potential candidate for xylene gas sensing.

Acknowledgements

The study was supported by National Natural Science Foundation of China (Grant No. 61404058, 51303061), National High Technology Research and Development Program of China (Grant No. 2013AA030902), Project of Science and Technology Plan of Changchun City (Grant No. 13KG49), and Post doctoral Sustentation Fund of Jilin Province(Grant No.RB201371).

Notes and references

[a]State Key Laboratory on Integrated Optoelectronics, Jilin University, Changchun 130012, China.
[b]College of Electronic Science and Engineering, Jilin University, Changchun 130012, China.

1. J. Hue, M. Dupoy, T. Bordy, R. Rousier, S. Vignoud, B. Schaerer, T. H. Tran-Thi, C. Rivron, L. Mugherli and P. Karpe, *Sensors and Actuators B: Chemical*, 2013, **189**, 194-198.
2. C. E. Davis, C. K. Ho, R. C. Hughes and M. L. Thomas, *Sensors and Actuators B: Chemical*, 2005, **104**, 207-216.
3. T. Akiyama, Y. Ishikawa and K. Hara, *Sensors and Actuators B: Chemical*, 2013, **181**, 348-352.
4. Y. Chen, L. Zhu, C. Feng, J. Liu, C. Li, S. Wen and S. Ruan, *Journal of Alloys and Compounds*, 2013, **581**, 653-658.
5. H.-M. Jeong, H.-J. Kim, P. Rai, J.-W. Yoon and J.-H. Lee, *Sensors and Actuators B: Chemical*, 2014, **201**, 482-489.

6. J. Park, G. Park, H.-J. Ko and J.-S. Ha, *Ceramics International*, 2014, **40**, 16281-16285.
7. Y. Ma, X. Zhang, M. Yang and Y. Qi, *Materials Letters*, 2014, **136**, 146-149.
8. N. Datta, N. S. Ramgir, S. Kumar, P. Veerender, M. Kaur, S. Kailasaganapathi, A. K. Debnath, D. K. Aswal and S. K. Gupta, *Sensors and Actuators B: Chemical*, 2014, **202**, 1270-1280.
9. M. Maniruzzaman, M. A. Rahman, K. Jeong, H.-s. Nam and J. Lee, *Renewable Energy*, 2014, **71**, 193-199.
10. Y. Meng, T. Wang, S. Chen, Y. Zhao, X. Ma and J. Gong, *Applied Catalysis B: Environmental*, 2014, **160-161**, 161-172.
11. Z. Zhang, R. Yang, Y. Gao, Y. Zhao, J. Wang, L. Huang, J. Guo, T. Zhou, P. Lu, Z. Guo and Q. Wang, *Scientific reports*, 2014, **4**, 6797.
12. Y. Wang, X. Zhang, Z. Luo, X. Huang, C. Tan, H. Li, B. Zheng, B. Li, Y. Huang, J. Yang, Y. Zong, Y. Ying and H. Zhang, *Nanoscale*, 2014, **6**, 12340-12344.
13. D. Wang, N. Liu, J. Zhang, X. Zhao, W. Zhang and M. Zhang, *Journal of Molecular Catalysis A: Chemical*, 2014, **393**, 47-55.
14. F. Jiang, W. Li, R. Zou, Q. Liu, K. Xu, L. An and J. Hu, *Nano Energy*, 2014, **7**, 72-79.
15. X. Zhang, X. Zeng, M. Yang and Y. Qi, *ACS applied materials & interfaces*, 2014, **6**, 1125-1130.
16. C. Liu, Z. Li and Z. Zhang, *Electrochimica Acta*, 2014, **134**, 84-91.
17. Z. Hongmei, X. Jianjian, Z. wenjin and H. Wei, *Displays*, 2014, **35**, 171-175.
18. Z. Yin, X. Zhang, Y. Cai, J. Chen, J. I. Wong, Y. Y. Tay, J. Chai, J. Wu, Z. Zeng, B. Zheng, H. Y. Yang and H. Zhang, *Angewandte Chemie*, 2014, **53**, 12560-12565.
19. S. Bai, S. Chen, L. Chen, K. Zhang, R. Luo, D. Li and C. C. Liu, *Sensors and Actuators B: Chemical*, 2012, **174**, 51-58.
20. A. D. Rushi, K. P. Datta, P. S. Ghosh, A. Mulchandani and M. D. Shirsat, *The Journal of Physical Chemistry C*, 2014, **118**, 24034-24041.
21. Y. H. Cho, Y. N. Ko, Y. C. Kang, I.-D. Kim and J.-H. Lee, *Sensors and Actuators B: Chemical*, 2014, **195**, 189-196.
22. W.-S. Kim, H.-C. Kim and S.-H. Hong, *Journal of Nanoparticle Research*, 2009, **12**, 1889-1896.
23. M. B. Rahmani, S. H. Keshmiri, J. Yu, A. Z. Sadek, L. Al-Mashat, A. Moafi, K. Latham, Y. X. Li, W. Wlodarski and K. Kalantar-zadeh, *Sensors and Actuators B: Chemical*, 2010, **145**, 13-19.
24. L. Wang, P. Gao, D. Bao, Y. Wang, Y. Chen, C. Chang, G. Li and P. Yang, *Crystal Growth & Design*, 2014, **14**, 569-575.
25. L. Brigo, M. Cittadini, L. Artiglia, G. A. Rizzi, G. Granozzi, M. Guglielmi, A. Martucci and G. Brusatin, *Journal of Materials Chemistry C*, 2013, **1**, 4252.
26. C. Feng, W. Li, C. Li, L. Zhu, H. Zhang, Y. Zhang, S. Ruan, W. Chen and L. Yu, *Sensors and Actuators B: Chemical*, 2012, **166-167**, 83-88.
27. L. Li, P. Gao, M. Baumgarten, K. Mullen, N. Lu, H. Fuchs and L. Chi, *Advanced materials*, 2013, **25**, 3419-3425.
28. F. Qu, C. Feng, C. Li, W. Li, S. Wen, S. Ruan and H. Zhang, *International Journal of Applied Ceramic Technology*, 2014, **11**, 619-625.